DOI: 10.3901/CJME.2015.0626.083, available online at www.springerlink.com; www.cjmenet.com; www.cjme.com.cn

Nonlinear Mathematical Modeling and Sensitivity Analysis of Hydraulic Drive Unit

KONG Xiangdong[1, 2], YU Bin[3, *], QUAN Lingxiao[1, 2], BA Kaixian[3], and WU Liujie[3]

1 *National Engineering Research Center for Local Joint of Advanced Manufacturing Technology and Equipment, Yanshan University, Qinhuangdao 066004, China*
2 *Hebei Provincial Key Laboratory of Heavy Machinery Fluid Power Transmission and Control, Yanshan University, Qinhuangdao 066004, China*
3 *School of Mechanical Engineering, Yanshan University, Qinhuangdao 066004, China*

Received December 19, 2014; revised June 15, 2015; accepted June 26, 2015

Abstract: The previous sensitivity analysis researches are not accurate enough and also have the limited reference value, because those mathematical models are relatively simple and the change of the load and the initial displacement changes of the piston are ignored, even experiment verification is not conducted. Therefore, in view of deficiencies above, a nonlinear mathematical model is established in this paper, including dynamic characteristics of servo valve, nonlinear characteristics of pressure-flow, initial displacement of servo cylinder piston and friction nonlinearity. The transfer function block diagram is built for the hydraulic drive unit closed loop position control, as well as the state equations. Through deriving the time-varying coefficient items matrix and time-varying free items matrix of sensitivity equations respectively, the expression of sensitivity equations based on the nonlinear mathematical model are obtained. According to structure parameters of hydraulic drive unit, working parameters, fluid transmission characteristics and measured friction-velocity curves, the simulation analysis of hydraulic drive unit is completed on the MATLAB/Simulink simulation platform with the displacement step 2 mm, 5 mm and 10 mm, respectively. The simulation results indicate that the developed nonlinear mathematical model is sufficient by comparing the characteristic curves of experimental step response and simulation step response under different constant load. Then, the sensitivity function time-history curves of seventeen parameters are obtained, basing on each state vector time-history curve of step response characteristic. The maximum value of displacement variation percentage and the sum of displacement variation absolute values in the sampling time are both taken as sensitivity indexes. The sensitivity indexes values above are calculated and shown visually in histograms under different working conditions, and change rules are analyzed. Then the sensitivity indexes values of four measurable parameters, such as supply pressure, proportional gain, initial position of servo cylinder piston and load force, are verified experimentally on test platform of hydraulic drive unit, and the experimental research shows that the sensitivity analysis results obtained through simulation are approximate to the test results. This research indicates each parameter sensitivity characteristics of hydraulic drive unit, the performance-affected main parameters and secondary parameters are got under different working conditions, which will provide the theoretical foundation for the control compensation and structure optimization of hydraulic drive unit.

Keywords: nonlinear mathematical model, hydraulic drive unit, valve-controlled symmetrical cylinder, sensitivity analysis, sensitivity index

1 Introduction

Relative to the wheeled robot and tracked robot, legged robot has better adaptability to unknown environments and attracts more and more attention among robotics researchers[1–2]. Among many kinds of maneuvering systems, hydraulic drive is regarded as an ideal joint drive with the advantages of small size, high output power, fast response and high precision[3–4].

However, the existing hydraulic drive unit brings some common hydraulic system problems, such as nonlinear phenomenon, parameter time-varying characteristic, coupled with complex and changeable load spectrum. All the factors above make hydraulic drive unit difficult to control.

Key nonlinear factors and time-varying parameters in hydraulic system influence the control characteristics obviously in the whole motion cycle. Grasping these factors and parameters is very significant to explore specific compensation control methods for improving

* Corresponding author. E-mail: yb@ysu.edu.cn
Supported by National Key Basic Research Program of China (973 Program, Grant No. 2014CB046405), Hebei Provincial Applied Basic Research Program (Grant No. 12962147D), National Natural Science Foundation of China (Grant No. 51375423)

control robustness of hydraulic drive unit. Sensitivity analysis is an effective way to analyze the degree of the parameter variation influencing system characteristics quantitatively, and it has been applied successfully in many fields recently, such as hydrology, hydraulics, power systems, mechanical design and reliability analysis, stability analysis, mechanical vibration transmission and control, and so on. SONG, et al[5], adopted sensitivity analysis to research uncertainty quantification of hydrological model, which can identify the dominant parameters to enhance the model optimization efficiency. JIM, et al[6], adopted global variance-based sensitivity analysis to research a simple pipe bend example and an advanced Shallow Water Equation solver, which can indicate this sensitivity analysis method is more general in its applicability and in its capacity to reflect nonlinear processes and the effects of interactions among variables. MIAO, et al[7], introduced the application status and development trend of the sensitivity analysis in power systems. JIN, et al[8] and WANG, et al[9], adopted sensitivity analysis method to discuss the variation regularities of reliability sensitivity, and analyzed the effect of design parameters on reliability of the bolt and the automobile front axle. ABOLFAZL, et al[10], adopted sensitivity analysis to find the influencing parameters of the stability of the underground rock structures for the best set of parameters. ZHOU, et al[11], used an improved analysis method for critical structures reliability analysis based on the failure assessment diagram. HISKENS, et al[12], adopted trajectory sensitivity analysis to research the jump conditions of switching and state resetting in the hybrid system. LIU, et al[13], used sensitivity analysis to research dynamic optimization design of supports' positions for engine pipelines. However, sensitivity analysis has relatively few applications in modeling and experimentof electro-hydraulic servo control system. VILENIUS[14] established a fifth-order electro-hydraulic position control system mathematical model which contained dead zone nonlinearity and pressure-flow nonlinearity of servo valve, and gave ten main parameters sensitivity analysis. FTARASA, et al[15], applied several sensitivity analysis methods, such as Vilenius Method, Revised Vilenius Method, Entirety-index Method and Individual Characteristics Method to linear mathematical model of hydraulic system, and analyzed advantages and disadvantages of these methods. KONG, et al[16], analyzed trajectory sensitivity of PID controls parameters and some structural parameters by modeling and simulation based on linear mathematical model of hydraulic drive unit of quadruped bionic robot. However, previous sensitivity analysis researches are not accurate enough, because those mathematical models were relatively simple and the change of the load and the initial displacement changes of servo piston were ignored, even experiment verification was not conducted.

In this paper, the seventeen parameters sensitivity equations are derived, basing on sixth-order nonlinear mathematical model of hydraulic drive unit. Then parameters sensitivity values and change rules of step response of piston displacement are obtained under different load force conditions. Finally nonlinear mathematical model of hydraulic drive unit and sensitivity indexes of a few measurable parameters are verified by experiment for ensuring accurate and practical of sensitivity analysis.

2 Nonlinear Mathematics Model of Hydraulic Drive Unit

2.1 Mathematical model and transfer block diagram

Hydraulic drive unit of legged robot is a small system of servo valve-controlled symmetrical cylinder. The principle of hydraulic drive unit is shown in Fig. 1.

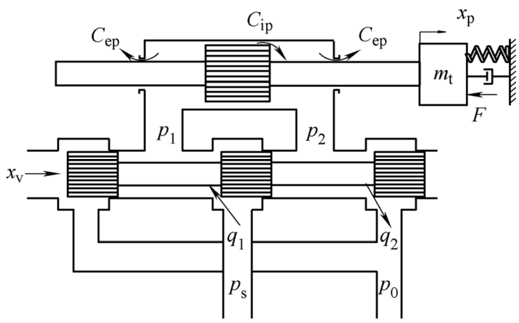

Fig. 1. Principle of hydraulic drive unit

According to the time domain and frequency domain characteristic curves in servo valve stylebook, servo valve can be equivalent to second-order oscillation link. Denote transfer function of input voltage of servo amplifier to spool displacement as follows:

$$\frac{X_v}{U_g}=\frac{K_{axv}}{\left(\dfrac{s^2}{\omega^2}+\dfrac{2\zeta}{\omega}s+1\right)}, \tag{1}$$

where K_{axv} is the servo valve gain, ζ is the damping ratio of servo valve, and ω is the natural frequency of servo valve.

The power stage structure of servo valve is equivalent to the ideal zero opening spool valve which has four matching and symmetrical orifices. Namely, the discharge coefficients of four orifices are equal, and pressure loss of the piping and valve chamber is much smaller than the throttling loss of valve port. And the pressure-flow nonlinearity of servo valve is necessary to be considered[17].

Denote inlet oil flow formula of servo valve:

$$q_1 = K_d \cdot x_v \cdot \sqrt{\left\{\frac{[1+\mathrm{sgn}(x_v)]p_s}{2}+\frac{[-1+\mathrm{sgn}(x_v)]p_0}{2}\right\}-\mathrm{sgn}(x_v)p_1}. \tag{2}$$

Denote outlet oil flow formula of servo valve:

$$q_2 = K_\mathrm{d} \bullet x_\mathrm{v} \bullet \sqrt{\left\{\frac{[1-\mathrm{sgn}(x_\mathrm{v})]p_\mathrm{s}}{2} + \frac{[-1-\mathrm{sgn}(x_\mathrm{v})]p_0}{2}\right\} + \mathrm{sgn}(x_\mathrm{v})\,p_2}, \tag{3}$$

where K_d is the conversion factor and $K_\mathrm{d} = C_\mathrm{d} W \sqrt{2/\rho}$, C_d is the spool valve orifice flow coefficient, ω is the area gradient, p_s is the supply pressure, p_0 is the return oil pressure, p_1 is the left cavity pressure of servo cylinder, and x_v is the spool displacement.

Considering the influence of servo cylinder leakage and oil compressibility, denote inlet oil flow formula and inlet oil cavity volume of servo cylinder:

$$\begin{cases} q_1 = A_\mathrm{p}\dfrac{\mathrm{d}x_\mathrm{p}}{\mathrm{d}t} + C_\mathrm{ip}(p_1 - p_2) + C_\mathrm{ep}p_1 + \dfrac{V_1}{\beta_\mathrm{e}}\dfrac{\mathrm{d}p_1}{\mathrm{d}t}, \\ V_1 = V_{01} + A_\mathrm{p}x_\mathrm{p}. \end{cases} \tag{4}$$

Denote outlet oil flow formula and inlet oil cavity volume of servo cylinder:

$$\begin{cases} q_2 = A_\mathrm{p}\dfrac{\mathrm{d}x_\mathrm{p}}{\mathrm{d}t} + C_\mathrm{ip}(p_1 - p_2) - C_\mathrm{ep}p_2 - \dfrac{V_2}{\beta_\mathrm{e}}\dfrac{\mathrm{d}p_2}{\mathrm{d}t}, \\ V_2 = V_{02} - A_\mathrm{p}x_\mathrm{p}, \end{cases} \tag{5}$$

where A_p is the servo cylinder piston area, x_p is the servo cylinder piston displacement, C_ip is the servo cylinder internal leakage coefficient, C_ep is the servo cylinder external leakage coefficient, β_e is the effective bulk modulus, V_{01} is the initial volume of inlet oil cavity, and V_{02} is the initial volume of outlet oil cavity.

Because $A_\mathrm{p}x_\mathrm{p}$ in Eq. (5) is not small enough to be ignored through being compared with V_{01} and V_{02}, considering the effect of the servo cylinder initial position variation on the volume change of servo cylinder inlet/outlet oil cavity could improve the model accuracy.

Denote V_{01} and V_{02} as follows:

$$\begin{cases} V_{01} = V_{\mathrm{g}1} + A_\mathrm{p}L_0, \\ V_{02} = V_{\mathrm{g}2} + A_\mathrm{p}(L - L_0), \end{cases} \tag{6}$$

where $V_{\mathrm{g}1}$ is the volume of inlet oil pipe, $V_{\mathrm{g}2}$ is the volume of outlet oil pipe, L is the stroke length of servo cylinder piston, and L_0 is the initial position of servo cylinder piston.

Taking the load characteristics of hydraulic drive unit into consider, the output force and load force of servo cylinder balance equation is determined as follows:

$$A_\mathrm{p}p_1 - A_\mathrm{p}p_2 = m_\mathrm{t}\frac{\mathrm{d}x_\mathrm{p}^2}{\mathrm{d}t} + B_\mathrm{p}\frac{\mathrm{d}x_\mathrm{p}}{\mathrm{d}t} + Kx_\mathrm{p} + F_\mathrm{f} + F, \tag{7}$$

where m_t is the total mass converted to the servo cylinder piston, B_p is the viscous damping, K is the load stiffness, F_f is the coulomb friction and F is the load force.

The transfer function of displacement sensor is proportional to its natural frequency, and its natural frequency is much bigger than system sampling frequency. Denote transfer function of servo cylinder piston displacement to feedback voltage:

$$\frac{U_\mathrm{p}}{X_\mathrm{p}} = K_\mathrm{x}, \tag{8}$$

where K_x is displacement sensor gain.

Integrating the equations from Eq. (1) to Eq. (8), the closed loop position control block diagram of hydraulic drive unit is shown in Fig. 2.

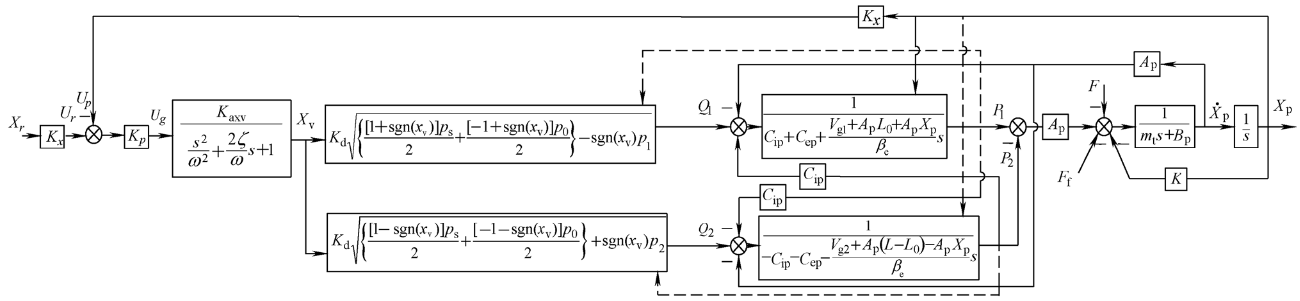

Fig. 2. Closed loop position control block diagram of hydraulic drive unit

2.2 State equations

General system state equations can be expressed as follows:

$$\dot{x} = f(\boldsymbol{x}, \boldsymbol{u}, \boldsymbol{\alpha}, t), \tag{9}$$

where $\boldsymbol{x}$ is the n-dimensional state vector, $\boldsymbol{u}$ is the r-dimensional input vector, $\boldsymbol{\alpha}$ is the p-dimensional parameter vector and t is the time.

From Fig. 2, the highest order of nonlinear mathematical model of hydraulic drive unit is sixth-order (n=6). Six state variables, one input and seventeen parameters (p=17) are selected.

Denote each vector of Eq. (9) as follows:

$$\boldsymbol{x} = [x_1, x_2, x_3, x_4, x_5, x_6]^\mathrm{T},\ \boldsymbol{u} = [u_1]^\mathrm{T},$$

$$\boldsymbol{\alpha}=[\alpha_1,\alpha_2,\alpha_3,\alpha_4,\alpha_5,\alpha_6,\alpha_7,\alpha_8,\alpha_9,\alpha_{10},\alpha_{11},\\ \alpha_{12},\alpha_{13},\alpha_{14},\alpha_{15},\alpha_{16},\alpha_{17}]^{\mathrm{T}},$$

where the state variables of state vector $\boldsymbol{x}$ are

$$x_1=x_{\mathrm{p}},x_2=\dot{x}_{\mathrm{p}},x_3=x_{\mathrm{v}},x_4=\dot{x}_{\mathrm{v}},x_5=p_1,\ x_6=p_2.$$

Input of the input vector $\boldsymbol{u}$ is

$$u_1=x_{\mathrm{r}}.$$

Parameters of parameter vector $\boldsymbol{\alpha}$ are as follows:

$$\alpha_1=\omega,\alpha_2=\xi,\alpha_3=K_{\mathrm{d}},\alpha_4=P_{\mathrm{s}},\alpha_5=P_0,\\ \alpha_6=C_{\mathrm{ip}},\alpha_7=L,\alpha_8=L_0,\alpha_9=A_{\mathrm{p}},\alpha_{10}=\beta_{\mathrm{e}},\\ \alpha_{11}=m_{\mathrm{t}},\alpha_{12}=K_{\mathrm{x}},\alpha_{13}=K_{\mathrm{p}},\alpha_{14}=K_{\mathrm{axv}},\alpha_{15}=K,\\ \alpha_{16}=B_{\mathrm{p}},\alpha_{17}=F.$$

Denote the expanded form of Eq. (9) as

$$\begin{cases}\dot{x}_1=x_2,\\ \dot{x}_2=-\dfrac{K}{m_{\mathrm{t}}}x_1-\dfrac{B_{\mathrm{p}}}{m_{\mathrm{t}}}x_2+\dfrac{A_{\mathrm{p}}}{m_{\mathrm{t}}}x_5-\dfrac{A_{\mathrm{p}}}{m_{\mathrm{t}}}x_6-\dfrac{F_{\mathrm{f}}+F}{m_{\mathrm{t}}},\\ \dot{x}_3=x_4,\\ \dot{x}_4=-K_{\mathrm{x}}K_{\mathrm{axv}}K_P\omega^2x_1-\omega^2x_3-2\zeta\omega x_4+\\ \qquad K_{\mathrm{axv}}K_{\mathrm{p}}K_{\mathrm{x}}\omega^2x_r,\\ \dot{x}_5=\beta_{\mathrm{e}}(V_{\mathrm{g}1}+A_{\mathrm{p}}L_0+A_{\mathrm{p}}x_1)^{-1}[-A_{\mathrm{p}}x_2+K_{\mathrm{d}}\times\\ \qquad\sqrt{\left\{\dfrac{[1+\mathrm{sgn}(x_3)]p_{\mathrm{s}}}{2}+\dfrac{[-1+\mathrm{sgn}(x_3)]p_0}{2}\right\}-\mathrm{sgn}(x_3)x_5}\times\\ \qquad x_3-(c_{\mathrm{ip}}+c_{\mathrm{ep}})x_5+c_{\mathrm{ip}}x_6],\\ \dot{x}_6=\beta_{\mathrm{e}}(V_{\mathrm{g}2}+A_{\mathrm{p}}(L-L_0)-A_{\mathrm{p}}x_1)^{-1}[A_{\mathrm{p}}x_2-K_{\mathrm{d}}\times\\ \qquad\sqrt{\left\{\dfrac{[1-\mathrm{sgn}(x_3)]p_{\mathrm{s}}}{2}+\dfrac{[-1-\mathrm{sgn}(x_3)]p_0}{2}\right\}+\mathrm{sgn}(x_3)x_6}\times\\ \qquad x_3+c_{\mathrm{ip}}x_5-(c_{\mathrm{ip}}+c_{\mathrm{ep}})x_6].\end{cases}$$

3 Sensitivity Equations of Hydraulic Drive Unit

3.1 General type of sensitivity equations

Compared with the high order sensitivity modeling and solution, the first order sensitivity model is sufficiently accuracy and relatively easier to solve. Therefore, the first order sensitivity model is selected for sensitivity analysis of hydraulic drive unit in this paper.

Denote the solution of Eq. (9) as

$$x_n(t)=\phi(t,\alpha_n),\ n=1,2,\cdots,6. \tag{10}$$

Denote sensitivity function of state vector with respect to parameter vector:

$$\lambda^i=\left(\frac{\partial x}{\partial\alpha_i}\right)_n,\ i=1,2,\cdots,17. \tag{11}$$

The initial conditions are

$$\lambda_0^i=\left(\frac{\partial x_0}{\partial\alpha_i}\right)_n,\ i=1,2,\cdots,17. \tag{12}$$

Assuming $\boldsymbol{u}$ is independent of $\boldsymbol{\alpha}$, denote the partial derivatives of Eq. (9) with respect to $\boldsymbol{\alpha}$ as follows:

$$\dot{\lambda}^i=\left(\frac{\partial f}{\partial x}\right)_n\lambda^i+\left(\frac{\partial f}{\partial\alpha_i}\right)_n,\ i=1,2,\cdots,17. \tag{13}$$

Eq. (13) are sensitivity equations, where $(\partial\boldsymbol{f}/\partial\boldsymbol{x})_n$ is coefficient matrix and $(\partial\boldsymbol{f}/\partial\alpha_i)_n$ is free matrix.

3.2 Calculation of coefficient matrix and free matrix

According to sensitivity Eq. (13), denote the partial derivatives of Eq. (9) with respect to state vector $\boldsymbol{x}$, and Jacobian matrix can be calculated as follows:

$$\frac{\partial f}{\partial x_1}=\Bigg[0,-\frac{K}{m_{\mathrm{t}}},0,-K_{\mathrm{x}}K_{\mathrm{axv}}K_{\mathrm{p}}\omega^2,\\ A_{\mathrm{p}}\beta_{\mathrm{e}}(V_{\mathrm{g}1}+A_{\mathrm{p}}L_0+A_{\mathrm{p}}x_1)^{-2}[A_{\mathrm{p}}x_2-\\ K_{\mathrm{d}}\sqrt{\left\{\frac{[1+\mathrm{sgn}(x_3)]p_{\mathrm{s}}}{2}+\frac{[-1+\mathrm{sgn}(x_3)]p_0}{2}\right\}-\mathrm{sgn}(x_3)x_5}\times\\ x_3+(c_{\mathrm{ip}}+c_{\mathrm{ep}})x_5-c_{\mathrm{ip}}x_6],\\ A_{\mathrm{p}}\beta_{\mathrm{e}}(V_{\mathrm{g}2}+A_p(L-L_0)-A_{\mathrm{p}}x_1)^{-2}[A_{\mathrm{p}}x_2-K_{\mathrm{d}}\times\\ \sqrt{\left\{\frac{[1-\mathrm{sgn}(x_3)]p_{\mathrm{s}}}{2}+\frac{[-1-\mathrm{sgn}(x_3)]p_0}{2}\right\}+\mathrm{sgn}(x_3)x_6}\times\\ x_3+c_{\mathrm{ip}}x_5-(c_{\mathrm{ip}}+c_{\mathrm{ep}})x_6\Bigg]^{\mathrm{T}},$$

$$\frac{\partial f}{\partial x_2}=\Bigg[1,-\frac{B_{\mathrm{p}}}{m_t},0,0,-\beta_{\mathrm{e}}A_{\mathrm{p}}(V_{\mathrm{g}1}+A_{\mathrm{p}}L_0+A_{\mathrm{p}}x_1)^{-1},\\ \beta_{\mathrm{e}}A_{\mathrm{p}}(V_{\mathrm{g}2}+A_p(L-L_0)-A_{\mathrm{p}}x_1)^{-1}\Bigg]^{\mathrm{T}},$$

$$\frac{\partial f}{\partial x_3}=[0,0,0,-\omega^2,K_{\mathrm{d}}\beta_{\mathrm{e}}(V_{\mathrm{g}1}+A_{\mathrm{p}}L_0+A_{\mathrm{p}}x_1)^{-1}\times\\ \sqrt{\left\{\frac{[1+\mathrm{sgn}(x_3)]p_{\mathrm{s}}}{2}+\frac{[-1+\mathrm{sgn}(x_3)]p_0}{2}\right\}-\mathrm{sgn}(x_3)x_5},\\ -K_{\mathrm{d}}\beta_{\mathrm{e}}(V_{\mathrm{g}2}+A_{\mathrm{p}}(L-L_0)-A_{\mathrm{p}}x_1)^{-1}\times\\ \sqrt{\left\{\frac{[1-\mathrm{sgn}(x_3)]p_{\mathrm{s}}}{2}+\frac{[-1-\mathrm{sgn}(x_3)]p_0}{2}\right\}+\mathrm{sgn}(x_3)x_6}\Bigg]^{\mathrm{T}}$$

$$\frac{\partial f}{\partial x_4}=[0,0,1,-2\zeta\omega,0,0]^{\mathrm{T}},$$

$$\frac{\partial f}{\partial x_5}=\left[0,\frac{A_{\mathrm{p}}}{m_{\mathrm{t}}},0,0,-\frac{1}{2}\mathrm{sgn}(x_3)K_{\mathrm{d}}\beta_{\mathrm{e}}\times\right.$$
$$(V_{\mathrm{g1}}+A_{\mathrm{p}}L_0+A_{\mathrm{p}}x_1)^{-1}x_3\times$$
$$\left\{\left\{\frac{[1+\mathrm{sgn}(x_3)]p_{\mathrm{s}}}{2}+\frac{[-1+\mathrm{sgn}(x_3)]p_0}{2}\right\}-\mathrm{sgn}(x_3)x_5\right\}^{-\frac{1}{2}}-$$
$$\beta_{\mathrm{e}}(c_{\mathrm{ip}}+c_{\mathrm{ep}})(V_{\mathrm{g1}}+A_{\mathrm{p}}L_0+A_{\mathrm{p}}x_1)^{-1},$$
$$\left.\beta_{\mathrm{e}}c_{\mathrm{ip}}(V_{\mathrm{g2}}+A_{\mathrm{p}}(L-L_0)-A_{\mathrm{p}}x_1)^{-1}\right]^{\mathrm{T}},$$

$$\frac{\partial f}{\partial x_6}=\left[0,-\frac{A_{\mathrm{p}}}{m_{\mathrm{t}}},0,0,\beta_{\mathrm{e}}c_{\mathrm{ip}}(V_{\mathrm{g1}}+A_{\mathrm{p}}L_0+A_{\mathrm{p}}x_1)^{-1},\right.$$
$$-\frac{1}{2}\mathrm{sgn}(x_3)K_{\mathrm{d}}\beta_{\mathrm{e}}(V_{\mathrm{g2}}+A_p(L-L_0)-A_{\mathrm{p}}x_1)^{-1}x_3\times$$
$$\left\{\left\{\frac{[1-\mathrm{sgn}(x_3)]p_{\mathrm{s}}}{2}+\frac{[-1-\mathrm{sgn}(x_3)]p_0}{2}\right\}+\mathrm{sgn}(x_3)x_6\right\}^{-\frac{1}{2}}-$$
$$\left.\beta_{\mathrm{e}}(c_{\mathrm{ip}}+c_{\mathrm{ep}})(V_{g2}+A_{\mathrm{p}}(L-L_0)-A_{\mathrm{p}}x_1)^{-1}\right]^{\mathrm{T}}. \tag{14}$$

The calculated sixth-order square matrix containing time-varying elements is coefficient matrix of $\boldsymbol{\lambda}^i$ in Eq. (13).

Then denote the partial derivatives of Eq. (9) with respect to parameter vector $\boldsymbol{\alpha}$, and the free matrix of sensitive equation can be obtained as follows:

$$\frac{\partial f}{\partial \alpha_1}=[0,0,0,-2K_{\mathrm{x}}K_{\mathrm{axv}}K_{\mathrm{P}}\omega x_1-2\omega x_3-$$
$$2\zeta x_4+2K_{\mathrm{axv}}K_{\mathrm{P}}K_{\mathrm{x}}\omega x_{\mathrm{r}},0,0]^{\mathrm{T}},$$

$$\frac{\partial f}{\partial \alpha_2}=\left[0,0,0,-2\omega x_4,0,0\right]^{\mathrm{T}},$$

$$\frac{\partial f}{\partial \alpha_3}=[0,0,0,0,\beta_{\mathrm{e}}(V_{\mathrm{g1}}+A_{\mathrm{p}}L_0+A_{\mathrm{p}}x_1)^{-1}x_3\times$$
$$\sqrt{\left\{\frac{[1+\mathrm{sgn}(x_3)]p_{\mathrm{s}}}{2}+\frac{[-1+\mathrm{sgn}(x_3)]p_0}{2}\right\}-\mathrm{sgn}(x_3)x_5},$$
$$-\beta_{\mathrm{e}}(V_{\mathrm{g2}}+A_{\mathrm{p}}(L-L_0)-A_{\mathrm{p}}x_1)^{-1}x_3\times$$
$$\left.\sqrt{\left\{\frac{[1-\mathrm{sgn}(x_3)]p_s}{2}+\frac{[-1-\mathrm{sgn}(x_3)]p_0}{2}\right\}+\mathrm{sgn}(x_3)x_6}\right]^{\mathrm{T}},$$

$$\frac{\partial f}{\partial \alpha_4}=\left[0,0,0,0,\frac{1+\mathrm{sgn}(x_3)}{4}K_{\mathrm{d}}\beta_{\mathrm{e}}(V_{\mathrm{g1}}+A_{\mathrm{p}}L_0+A_{\mathrm{p}}x_1)^{-1}\times\right.$$
$$\left\{\left\{\frac{[1+\mathrm{sgn}(x_3)]p_{\mathrm{s}}}{2}+\frac{[-1+\mathrm{sgn}(x_3)]p_0}{2}\right\}-\mathrm{sgn}(x_3)x_5\right\}^{-\frac{1}{2}}x_3,$$
$$-\frac{1-\mathrm{sgn}(x_3)}{4}K_{\mathrm{d}}\beta_{\mathrm{e}}(V_{\mathrm{g2}}+A_{\mathrm{p}}(L-L_0)-A_{\mathrm{p}}x)^{-1}x_3\times$$
$$\left.\left\{\left\{\frac{[1-\mathrm{sgn}(x_3)]p_s}{2}+\frac{[-1-\mathrm{sgn}(x_3)]p_0}{2}\right\}+\mathrm{sgn}(x_3)x_6\right\}^{-\frac{1}{2}}\right]^{\mathrm{T}},$$

$$\frac{\partial f}{\partial \alpha_5}=\left[0,0,0,0,\frac{-1+\mathrm{sgn}(x_3)}{4}K_{\mathrm{d}}\beta_{\mathrm{e}}(V_{\mathrm{g1}}+A_{\mathrm{p}}L_0+A_{\mathrm{p}}x_1)^{-1}\times\right.$$
$$\left\{\left\{\frac{[1+\mathrm{sgn}(x_3)]p_{\mathrm{s}}}{2}+\frac{[-1+\mathrm{sgn}(x_3)]p_0}{2}\right\}-\mathrm{sgn}(x_3)x_5\right\}^{-\frac{1}{2}}x_3,$$
$$-\frac{-1-\mathrm{sgn}(x_3)}{4}K_{\mathrm{d}}\beta_{\mathrm{e}}(V_{\mathrm{g2}}+A_{\mathrm{p}}(L-L_0)-A_{\mathrm{p}}x_1)^{-1}x_3\times$$
$$\left.\left\{\left\{\frac{[1-\mathrm{sgn}(x_3)]p_{\mathrm{s}}}{2}+\frac{[-1-\mathrm{sgn}(x_3)]p_0}{2}\right\}+\mathrm{sgn}(x_3)x_6\right\}^{-\frac{1}{2}}\right]^{\mathrm{T}},$$

$$\frac{\partial f}{\partial \alpha_6}=[0,0,0,0,(V_{\mathrm{g1}}+A_pL_0+A_{\mathrm{p}}x_1)^{-1}\beta_{\mathrm{e}}(-x_5+x_6),$$
$$(V_{\mathrm{g2}}+A_{\mathrm{p}}(L-L_0)-A_{\mathrm{p}}x_1)^{-1}\beta_{\mathrm{e}}(x_5-x_6)]^{\mathrm{T}},$$

$$\frac{\partial f}{\partial \alpha_7}=[0,0,0,0,0,-A_{\mathrm{p}}\beta_{\mathrm{e}}\times$$
$$(V_{\mathrm{g2}}+A_{\mathrm{p}}(L-L_0)-A_{\mathrm{p}}x_1)^{-2}[A_{\mathrm{p}}x_2-K_{\mathrm{d}}x_3\times$$
$$\sqrt{\left\{\frac{[1-\mathrm{sgn}(x_3)]p_s}{2}+\frac{[-1-\mathrm{sgn}(x_3)]p_0}{2}\right\}+\mathrm{sgn}(x_3)x_6}+$$
$$c_{\mathrm{ip}}x_5-(c_{\mathrm{ip}}+c_{\mathrm{ep}})x_6]]^{\mathrm{T}},$$

$$\frac{\partial f}{\partial \alpha_8}=[0,0,0,0,-A_{\mathrm{p}}\beta_{\mathrm{e}}\times$$
$$(V_{\mathrm{g1}}+A_{\mathrm{p}}L_0+A_{\mathrm{p}}x_1)^{-2}[-A_{\mathrm{p}}x_2+K_{\mathrm{d}}x_3\times$$
$$\sqrt{\left\{\frac{[1+\mathrm{sgn}(x_3)]p_{\mathrm{s}}}{2}+\frac{[-1+\mathrm{sgn}(x_3)]p_0}{2}\right\}-\mathrm{sgn}(x_3)x_5}-$$
$$(c_{\mathrm{ip}}+c_{\mathrm{ep}})x_5+c_{\mathrm{ip}}x_6],$$
$$A_{\mathrm{p}}\beta_{\mathrm{e}}(V_{\mathrm{g2}}+A_{\mathrm{p}}(L-L_0)-A_{\mathrm{p}}x_1)^{-2}[A_{\mathrm{p}}x_2-K_{\mathrm{d}}x_3\times$$
$$\sqrt{\left\{\frac{[1-\mathrm{sgn}(x_3)]p_{\mathrm{s}}}{2}+\frac{[-1-\mathrm{sgn}(x_3)]p_0}{2}\right\}+\mathrm{sgn}(x_3)x_6}+$$
$$c_{\mathrm{ip}}x_5-(c_{\mathrm{ip}}+c_{\mathrm{ep}})x_6]]^{\mathrm{T}},$$

$$\frac{\partial f}{\partial \alpha_9}=\left[0,\frac{x_5}{m_{\mathrm{t}}}-\frac{x_6}{m_{\mathrm{t}}},0,0,-\beta_{\mathrm{e}}x_2(V_{\mathrm{g1}}+A_{\mathrm{p}}L_0+A_{\mathrm{p}}x_1)^{-1}-\right.$$
$$\beta_{\mathrm{e}}(L_0+x_1)(V_{\mathrm{g1}}+A_{\mathrm{p}}L_0+A_{\mathrm{p}}x_1)^{-2}[-A_{\mathrm{p}}x_2+K_{\mathrm{d}}x_3\times$$
$$\sqrt{\left\{\frac{[1+\mathrm{sgn}(x_3)]p_s}{2}+\frac{[-1+\mathrm{sgn}(x_3)]p_0}{2}\right\}-\mathrm{sgn}(x_3)x_5}-$$
$$(c_{\mathrm{ip}}+c_{\mathrm{ep}})x_5+c_{\mathrm{ip}}x_6],\beta_{\mathrm{e}}x_2(V_{\mathrm{g2}}+A_{\mathrm{p}}(L-L_0)-A_{\mathrm{p}}x_1)^{-1}-$$
$$\beta_{\mathrm{e}}(L-L_0-x_1)(V_{\mathrm{g2}}+A_{\mathrm{p}}(L-L_0)-A_{\mathrm{p}}x_1)^{-2}[A_{\mathrm{p}}x_2-K_{\mathrm{d}}x_3\times$$
$$\sqrt{\left\{\frac{[1-\mathrm{sgn}(x_3)]p_{\mathrm{s}}}{2}+\frac{[-1-\mathrm{sgn}(x_3)]p_0}{2}\right\}+\mathrm{sgn}(x_3)x_6}+$$
$$c_{\mathrm{ip}}x_5-(c_{\mathrm{ip}}+c_{\mathrm{ep}})x_6]]^{\mathrm{T}},$$

$$\frac{\partial f}{\partial \alpha_{10}}=[0,0,0,0,(V_{g1}+A_pL_0+A_px_1)^{-1}[-A_px_2+K_dx_3\times$$
$$\sqrt{\left\{\frac{[1+\mathrm{sgn}(x_3)]p_s}{2}+\frac{[-1+\mathrm{sgn}(x_3)]p_0}{2}\right\}-\mathrm{sgn}(x_3)x_5}-$$
$$(c_{ip}+c_{ep})x_5+c_{ip}x_6],$$
$$(V_{g2}+A_p(L-L_0)-A_px_1)^{-1}[A_px_2-K_dx_3\times$$
$$\sqrt{\left\{\frac{[1-\mathrm{sgn}(x_3)]p_s}{2}+\frac{[-1-\mathrm{sgn}(x_3)]p_0}{2}\right\}+\mathrm{sgn}(x_3)x_6}+$$
$$c_{ip}x_5-(c_{ip}+c_{ep})x_6]]^{\mathrm{T}},$$

$$\frac{\partial f}{\partial \alpha_{11}}=\left[0,\frac{K}{m_t^2}x_1+\frac{B_p}{m_t^2}x_2-\frac{A_p}{m_t^2}x_5+\frac{A_p}{m_t^2}x_6+\frac{F_f+F}{m_t^2},0,0,0,0\right]^{\mathrm{T}},$$

$$\frac{\partial f}{\partial \alpha_{12}}=\left[0,0,0,-K_{axv}K_P\omega^2x_1+K_{axv}K_P\omega^2x_r,0,0\right]^{\mathrm{T}},$$

$$\frac{\partial f}{\partial \alpha_{13}}=\left[0,0,0,-K_xK_{axv}\omega^2x_1+K_{axv}K_x\omega^2x_r,0,0\right]^{\mathrm{T}},$$

$$\frac{\partial f}{\partial \alpha_{14}}=\left[0,0,0,-K_xK_P\omega^2x_1+K_PK_x\omega^2x_r,0,0\right]^{\mathrm{T}},$$

$$\frac{\partial f}{\partial \alpha_{15}}=\left[0,-\frac{1}{m_t}x_1,0,0,0,0\right]^{\mathrm{T}},$$

$$\frac{\partial f}{\partial \alpha_{16}}=\left[0,-\frac{1}{m_t}x_2,0,0,0,0\right]^{\mathrm{T}},$$

$$\frac{\partial f}{\partial \alpha_{17}}=\left[0,-\frac{1}{m_t},0,0,0,0\right]^{\mathrm{T}}. \qquad (15)$$

Since the mathematical model of hydraulic drive unit is based on increment equations, initial displacement of servo valve core and initial pressure of servo cylinder cavity are equal to 0 when t=0. Initial value of state vector $\boldsymbol{x}$ can be expressed as $\boldsymbol{x}_0=\boldsymbol{0}$.

According to Eq. (12), initial value of sensitivity function λ^i can be obtained as follows:

$$\lambda_0^i=0,\ i=1,2,\cdots,17. \qquad (16)$$

4 Sensitivity Analysis and Experiment of Hydraulic Drive Unit

4.1 Simulation and experimental verification of displacement step response

The dynamic characteristic test platform schematic of hydraulic drive unit is shown in Fig. 3. The left part is the tested hydraulic drive unit consisting of a small servo valve (200-0029, Star, UK), a servo cylinder, a displacement sensor and a force sensor, where the closed loop position control is adopted. The right part is load simulation section consisting of the same servo valve and servo cylinder, where the closed loop force control is adopted. Two cylinder rods are jointed rigidly by thread of force sensor. The experimental setup of test platform is shown in Fig. 4.

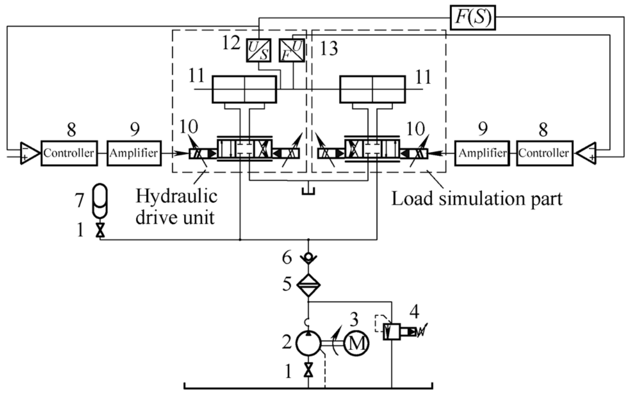

Fig. 3. Schematics of dynamic performance test platform of hydraulic drive unit

1. Globe valve; 2. Axial piston pump; 3. Electromotor; 4. Relief valve; 5. High-pressure filter; 6. Check valve; 7. Accumulator; 8. dSPACE controller; 9. Servo valve amplifier; 10. Servo valve; 11. Servo cylinder; 12. Displacement sensor; 13. Force sensor

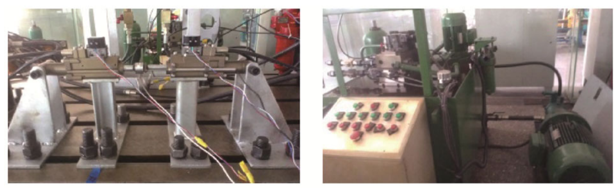

(a) Servo valves and actuators　　(b) Pump station

Fig. 4. Experimental setup of hydraulic drive unit test platform

The dSPACE semi-physical simulation device, which can connect with MATLAB/Simulink seamlessly, is used as controller of this test platform. Fig. 5 shows the dSPACE controller and operation interface. Real-time control, online detection and data acquisition are accomplished by using this simulation system.

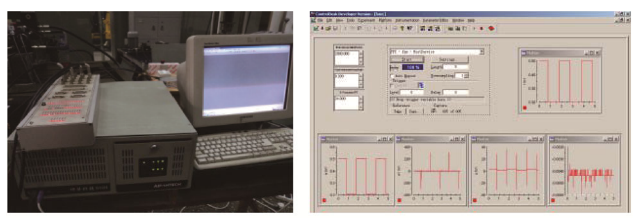

(a) dSPACE controller　　(b) Operation interface

Fig. 5. Controllers and operation interface of hydraulic drive unit test platform

The simulation model of transfer function of hydraulic drive (as denoted in Fig. 2) is built in MATLAB/Simulink environment. The structure parameters of servo cylinder, such as piston area, stroke length, and internal volume of servo cylinder, are established by physical structure of hydraulic drive unit. The working parameters, such as supply oil pressure, return oil pressure, and sensor gain, are established by experimental setup. The friction-speed characteristic curve of servo cylinder is obtained by repeated test and inputted into the simulation model. The natural frequency, damping and conversion factor of servo valve are got form dynamic characteristic test curves in the stylebook. Other parameters are estimated referring to actual working conditions of legged robot joints and engineering experience. These parameters and initial values of simulation model are listed in Table 1.

Compared with sine response curve and slope response curve, step response curves can intuitively reflect response rate, overshoot and steady-state error of hydraulic actuators, thus dynamic characteristics of hydraulic drive unit are evaluated by displacement step response curves in this paper. Giving displacement step values 2 mm, 5 mm and 10 mm, respectively, simulation and experimental curves of position closed loop control are shown in Fig. 6 under load 0 N, 500 N and 1000 N, respectively. It can be seen that simulation curves are close to experimental curves. The accuracy of simulation model can be proved by comparing theoretical step responses with experimental data. In other words, this nonlinear mathematical model and parameters settings are comparatively correct in these experimental conditions.

Table 1. Simulation model parameters and initial values

Simulation model parameter	Initial value
Servo valve gain K_{axv}/(mm • V^{-1})	0.45
Natural frequency of servo valve ω/(rad • s^{-1})	628
Damping ratio of servo valve ζ	0.77
Servo cylinder piston area A_p/cm^2	3.368
volume of input oil pipe V_{g1}/cm^3	0.62
volume of output oil pipe V_{g2}/cm^3	0.86
Total stroke of servo cylinder L/m	0.05
Initial position of servo cylinder piston L_0/m	0.02
Supply oil pressure p_s/MPa	7
Return oil pressure p_0/MPa	0.5
Proportional gain K_P	30
Displacement sensor gain K_x/(V • m^{-1})	182
External leakage coefficient C_{ep}/(m^3 • s^{-1} • Pa^{-1})	0
Internal leakage coefficient C_{ip}/(m^3 • s^{-1} • Pa^{-1})	2.38×10^{-13}
Total mass converted to servo cylinder piston m_t/kg	1.131 5
Effective bulk modulus β_e/MPa	800
Load stiffness K/(kN • m^{-1})	10
Viscous damping coefficient Bp/(kN • (m • s^{-1})$^{-1}$)	1
Conversion factor K_d/(cm^2 • s^{-1})	1.248

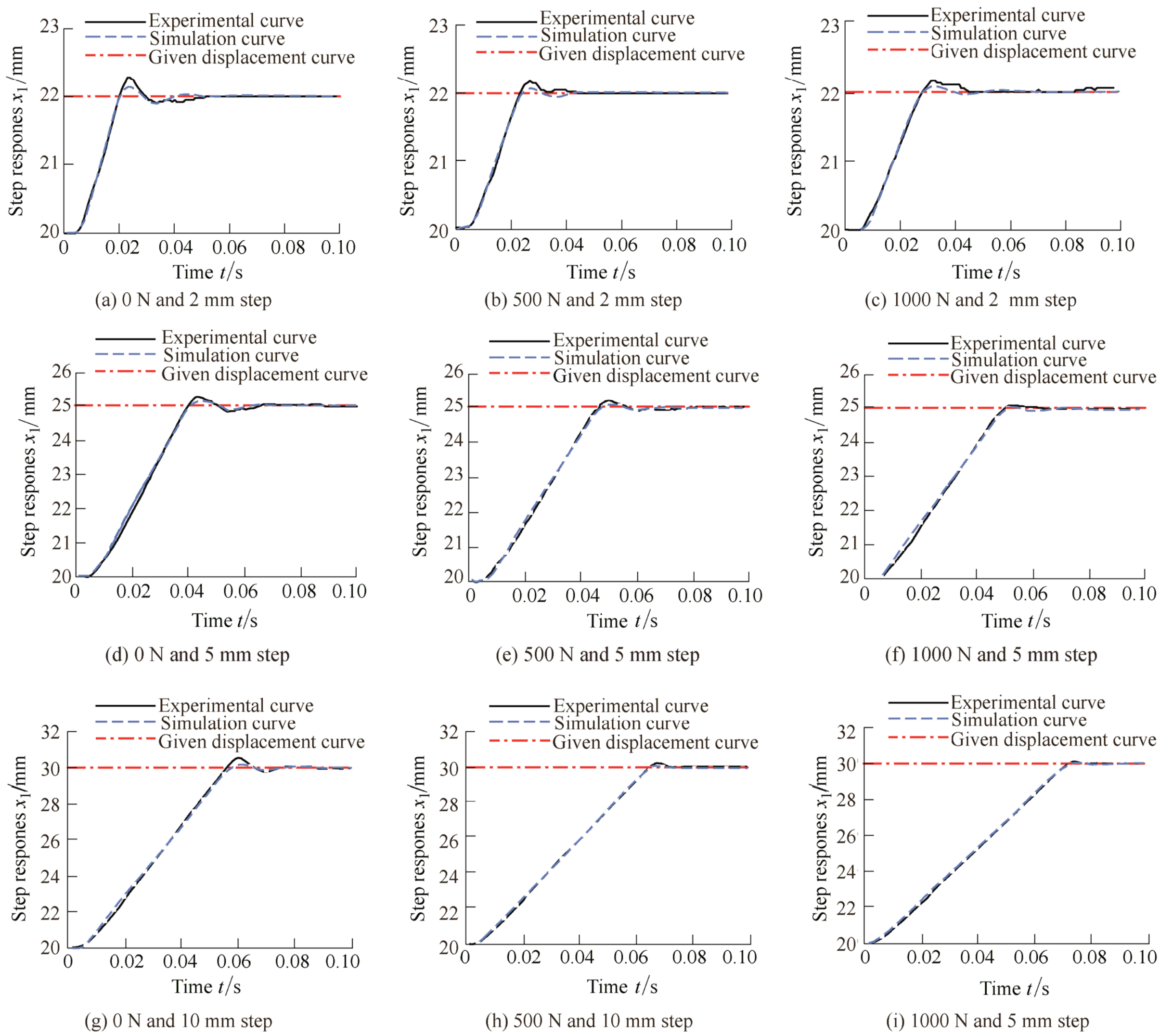

(a) 0 N and 2 mm step (b) 500 N and 2 mm step (c) 1000 N and 2 mm step

(d) 0 N and 5 mm step (e) 500 N and 5 mm step (f) 1000 N and 5 mm step

(g) 0 N and 10 mm step (h) 500 N and 10 mm step (i) 1000 N and 5 mm step

Fig. 6. Simulation and experimental curves of the servo cylinder displacement step response

4.2 Calculation of sensitivity function

The sensitivity Eq. (13) are first-order linear differential equations with time-varying coefficient matrix and free matrix. There are $n\times(p+1)$ equations consisting of n state variable equations and $n\times p$ sensitivity equations. Position control characteristic of the hydraulic drive unit is the major concern in this paper, therefore we only analyze the sensitivity of displacement step response x_1 for the parameter vector $\boldsymbol{\alpha}$.

By using fourth/fifth-order Runge-Kutta algorithm[18], Eq. (13) can be programmed for obtaining sensitivity function(S.F.) curves in MATLAB environment. The S.F. curves are shown in Fig. 7 under the load force of 0 N and displacement step of 2 mm.

Fig. 7. S.F. curves with 0 N and 2 mm step

Similarly, S.F. curves of different displacement steps and load forces should also be solved in order to research sensitivity values and change rules of state vector x_1 with respect to parameter vector $\boldsymbol{\alpha}$.

4.3 Sensitivity analysis

4.3.1 Sensitivity indexes

Due to parameter vector change $\Delta\boldsymbol{\alpha}$ causing state vector change $\Delta\boldsymbol{x}$, Eq. (10) is written by Taylor's theorem as follows:

$$\Delta\boldsymbol{x}=\left(\frac{\partial\boldsymbol{x}}{\partial\boldsymbol{\alpha}}\right)_n\Delta\boldsymbol{\alpha}+\text{high order terms},\tag{17}$$

where $(\partial\boldsymbol{x}/\partial\boldsymbol{\alpha})_n$ is sensitivity functions λ.

In order to evaluate quantitative impact of the state vector with respect to parameter change intuitively, the percentage Φ_p of $\Delta x_j / x_{sj}$ is used, where x_{sj} is steady-state difference value of input displacement and output displacement. Ignore high order terms and Eq. (17) can be transformed as follows:

$$\Phi_p = \frac{\Delta x_j}{x_{sj}} \times 100\% = \frac{\lambda_j^i \Delta \alpha_i}{x_{sj}} \times 100\%. \tag{18}$$

In order to show the sensitivity clearly, the maximum value of this percentage in Eq. (18) is defined as the first sensitivity index.

First sensitivity index can express the maximum value of impacts of parameters change with respect to x_1 in whole sampling time.

In order to evaluate the total impacts, the value I_s of whole sampling time integral $\left|(\partial x / \partial \alpha)_n\right| \Delta \alpha$ is defined as the second sensitivity index, and this index can be calculated as follows:

$$I_s = \int_0^t \left| \left(\frac{\partial x}{\partial \alpha} \right)_n \right| \Delta \alpha \, \mathrm{d} t. \tag{19}$$

4.3.2 Sensitivity analysis of no load

In the case of each parameter has 10% variation, and the displacement step of hydraulic drive unit is 2 mm without load, the percentage of time-history curves of state vector change $\Delta \boldsymbol{x}$ with respect to parameter vector change $\Delta \boldsymbol{\alpha}$ is shown in Fig. 8.

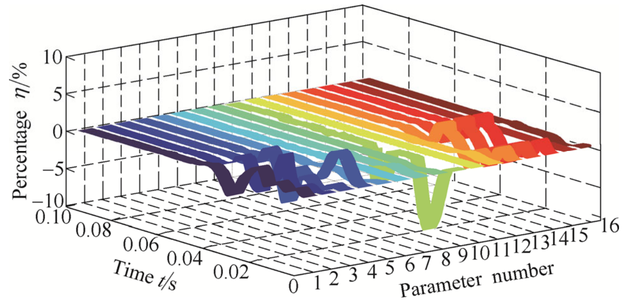

Fig. 8. Percentage of time-history curves with 2 mm displacement step without load

Similarly, the percentage of the curves can be solved as displacement steps of hydraulic drive unit are 5 mm and 10 mm without load. According to these curves, the histograms of first sensitivity index and second sensitivity index are shown in Fig. 9.

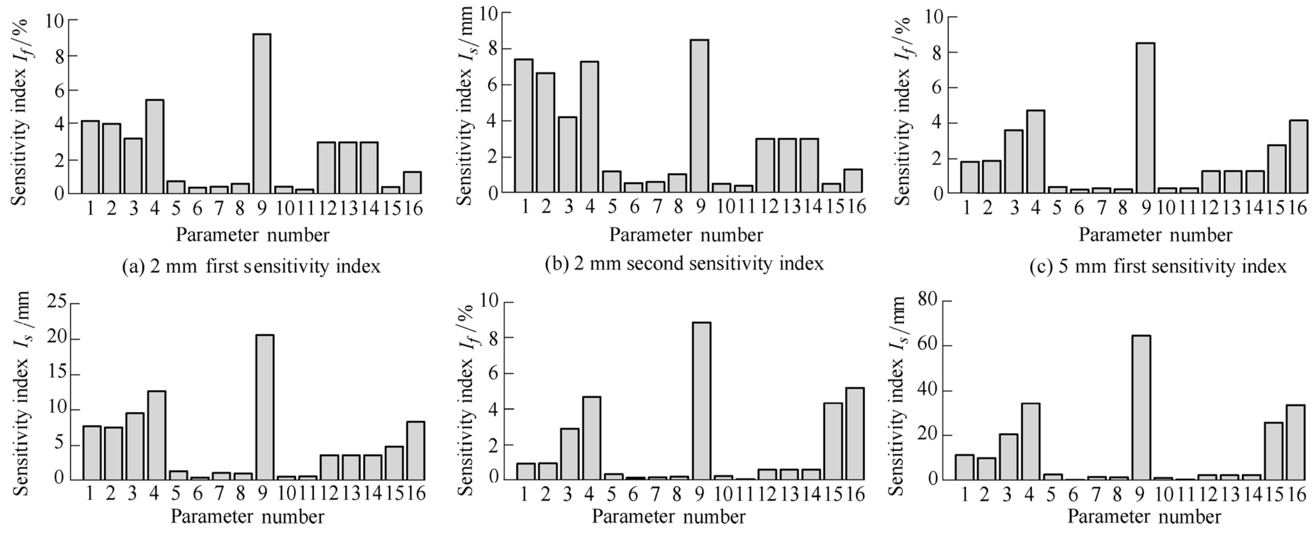

Fig. 9. Histograms of first sensitivity index and second sensitivity without load and different input steps

The values and change rules of two sensitivity indexes of each parameter can be described with the increase of displacement step value as follows.

For parameters α_5, α_6, α_7, α_8, α_{10} and α_{11}, i.e., return oil pressure, servo cylinder internal leakage coefficient, piston stroke of servo cylinder, initial position of servo cylinder piston, effective bulk modulus and total mass converted to servo cylinder piston, the values of first sensitivity index are all within 1%, and the proportions of second sensitivity index with respect to vertical axis in histograms is also quite small. So it is obvious that the change of these parameters has little effects on displacement output response x_1.

For parameters α_3, α_4 and α_9, i.e., conversion factor, supply oil pressure and servo cylinder piston area, the proportions of two sensitivity indexes basically remain the similar variation rule. These parameters' first sensitivity index is about 3%, 5% and 8%, respectively, and the values of second sensitivity index with respect to maximum values of vertical axis are orderly increasing with increasing of displacement step value. So these parameters have big effects on displacement output response x_1.

For parameters α_{12}, α_{13} and α_{14}, i.e., displacement sensor gain, proportional gain and servo valve gain, they have the same effects on displacement output response x_1. For parameters α_1 and α_2, i.e., natural frequency and damping ratio of servo valve, the proportions of two sensitivity indexes are relatively large with small displacement step value. The proportions of two sensitivity indexes of these five parameters above are inversely proportional to displacement step value. As the displacement step value is 2 mm, values of first sensitivity index of parameter α_1 and α_2 are about 4%, and they are slightly larger than those of parameters α_{12}, α_{13} and α_{14}.

For parameters α_{15} and α_{16}, i.e., load stiffness and viscous damping, the proportions of two sensitivity indexes remain increase with the increasing of displacement step value. As displacement step value is 2 mm, values of first sensitivity index are within 1% and 2%, respectively. As displacement step value is 5 mm, the values are about 3% and 4%, respectively. As displacement step value is 10 mm, the values are about 4% and 5%, respectively.

4.3.3 Sensitivity analysis of load

With different working conditions of legged robots, such as walking, trotting, jumping, and so on, load force values of hydraulic drive unit can vary greatly. So researching the sensitivity of x_1 with respect to each parameter is practically significant when load force changes.

As displacement step values are 2 mm, 5 mm and 10 mm, the histograms of two sensitivity indexes with 500 N and 1000 N constant load force are shown in Fig. 10 and Fig. 11, respectively.

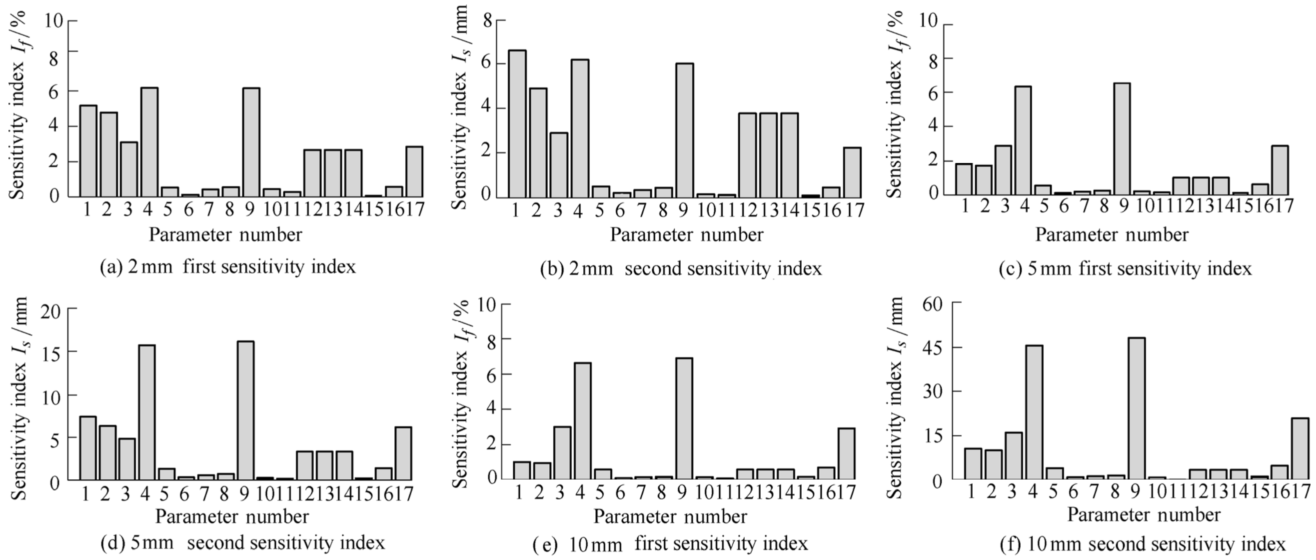

Fig. 10. Histograms of first sensitivity index and second sensitivity with 500 N load force

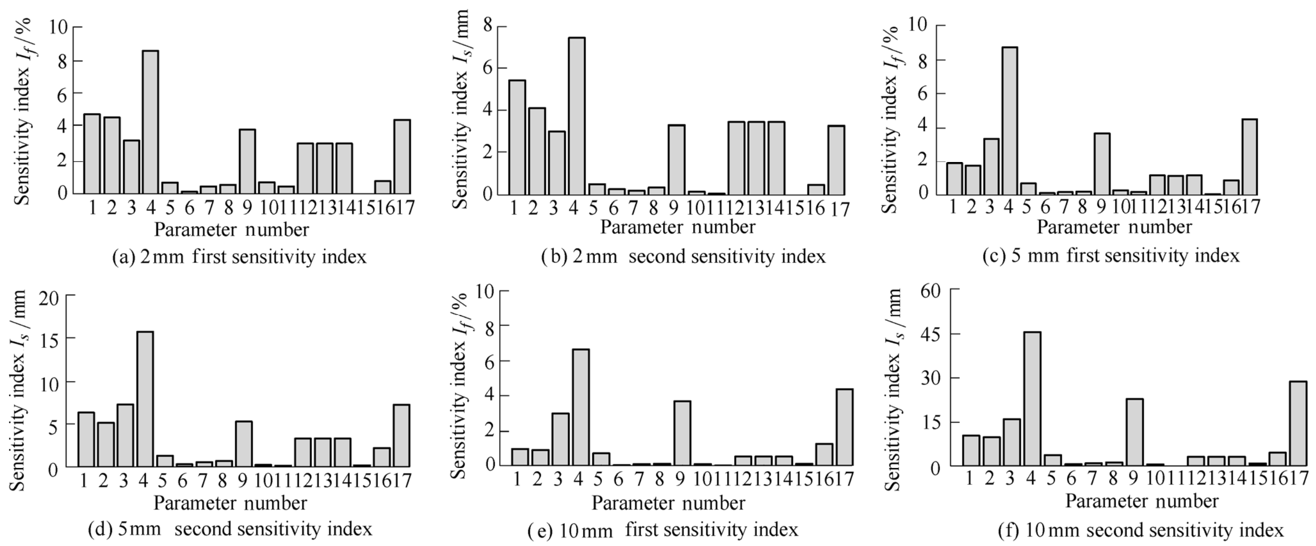

Fig. 11. Histograms of first sensitivity index and second sensitivity with 1000 N load force

It can be observed that two sensitivity indexes of most parameters under load are similar to those under no load, but the indexes of rest of parameters in load case are changing in varying degrees.

For parameters α_5, α_6, α_7, α_8, α_{10}, α_{11}, α_{15} and α_{16}, i.e., return oil pressure, servo cylinder internal leakage coefficient, piston stroke of servo cylinder piston, initial position of servo cylinder piston, effective bulk modulus, total mass converted to servo cylinder piston, load stiffness and viscous damping, these parameters' values of first sensitivity index are all within 1% and the proportions of second sensitivity index are also very small with 500 N and 1000 N load. So these parameters have few effects on x_1. Especially, for two sensitivity indexes of the parameter α_{15} and α_{16}, the proportions no longer increase with the increasing of displacement step value but are basically unchanged.

For parameters α_1, α_2, α_3, α_4, α_9, α_{12}, α_{13} and α_{14}, i.e., natural frequency of servo valve, damping ratio of servo valve, conversion factor, supply oil pressure, servo cylinder piston area, displacement sensor gain, proportional gain and servo valve gain, change rules of two sensitivity indexes are similar to those under no load. Especially, the proportions of two sensitivity indexes of parameter α_4 grow larger with the increasing of load F. As load F is 500 N, first sensitivity index of α_4 is approximately equal to 6%. When load F is 1000 N, two sensitivity indexes of α_4 are larger than those of any other parameters, thus α_4 among all the parameters has biggest effect on x_1. The proportions of two sensitivity indexes of parameter α_9 decrease with increasing of load F. As load F is 500 N, first sensitivity index of α_9 is approximately equal to α_4. When load F is 1000 N, first sensitivity index of α_9 is less than 4%. Two sensitivity indexes of the other parameters above have no obvious change with increasing of load F.

Furthermore, for parameter α_{17}, i.e., load force, its two sensitivity indexes have similar change rules with different initial load F. In the case of 500 N load, the proportions of two sensitivity indexes are basically unchanged with the increasing of displacement step, and they increase with the increasing load F. First sensitivity index is around 3% with 500 N load, and it is approximately 5% when load is 1000 N.

4.4 Experiment of sensitivity indexes

In order to verify the values and change rules of parameters sensitivity partly, four representative and measurable parameters α_8, α_8, α_{13} and α_{17} are taken as variables to obtain the experimental displacement output response x_1 by using dynamic characteristics test platform of hydraulic drive unit. Experimental conditions and methods are as follows.

Input displacement step values of 2 mm, 5 mm and 10 mm respectively, then adjust each parameter with 10% variation, i.e., proportional gain K_p from 40 to 36 or 44, initial position of servo cylinder piston L_0 from 20 mm to 18 mm or 22 mm, load F from 500 N to 450 N or 550 N, and 1000 N to 900 N or 1100 N. Output of displacement response of hydraulic drive unit is recorded respectively. Then samples averaging method is used to ensure the accuracy of experimental data. The comparative histograms of experimental and theoretical sensitivity indexes are shown in Fig. 12.

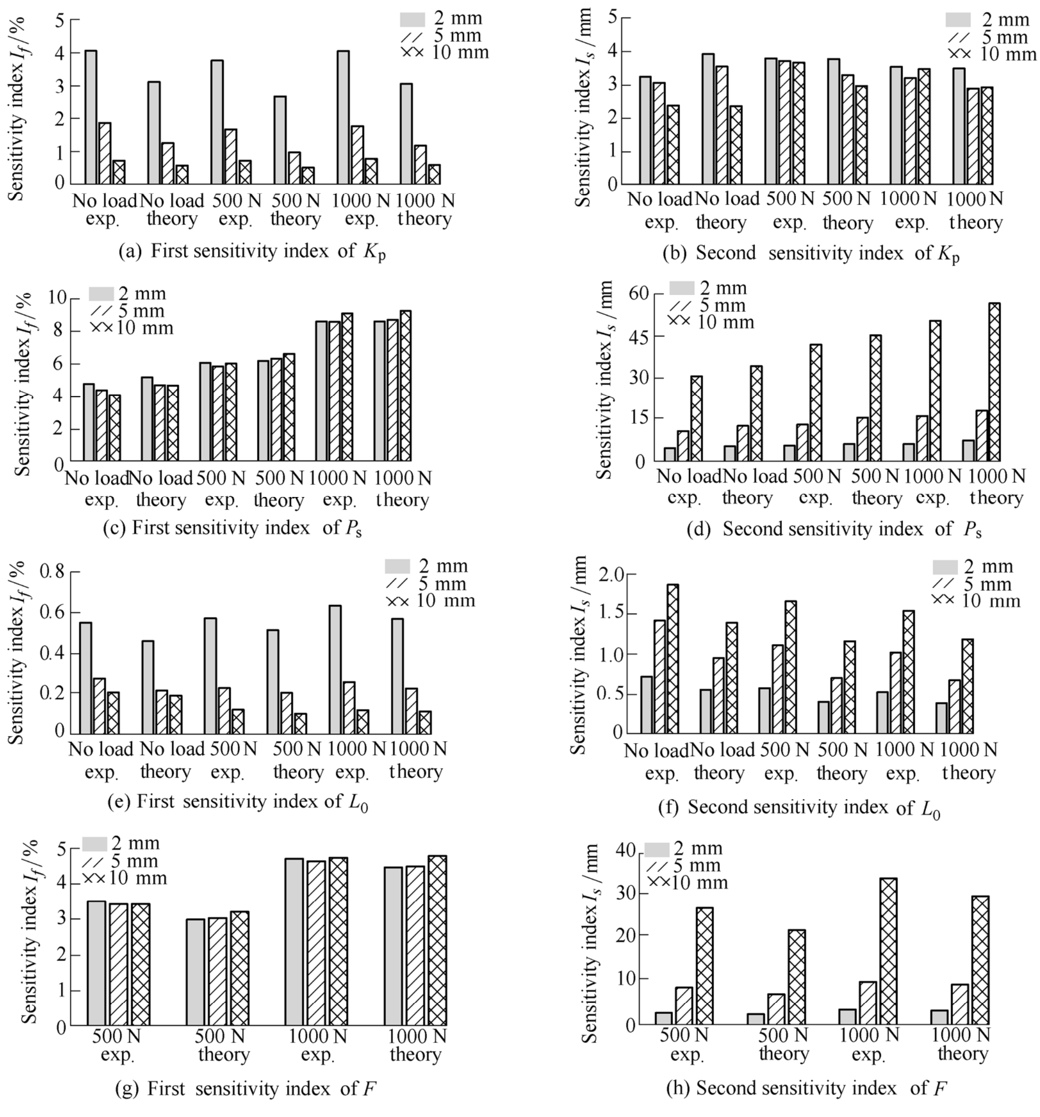

Fig. 12. Contrastive histograms of experimental and theoretical sensitivity indexes

It can be observed that the experimental values and change rules of two sensitivity indexes of these four parameters are similar to the theoretical ones, so the accuracy of theoretical analysis can be proved.

5 Conclusions

The influence degree and rules of10% parameters change with respect to displacement output response are obtained quantitatively by sensitivity analysis method, and the conclusions can be described as follows.

(1) Through theory research and experimental verification of the nonlinear mathematical modeling and some parameters sensitivity indexes, it is proved that the nonlinear mathematical modeling and sensitivity equations which contain dynamic characteristics of servo valve, nonlinear characteristics of pressure-flow, initial displacement of servo cylinder piston and friction nonlinearity are accuracy and can represent dynamic characteristics of hydraulic drive unit. So all the analysis results based on this nonlinear model can provide credible theoretical foundation for parameters optimization design and control compensation of hydraulic drive unit.

(2) For return oil pressure, servo cylinder internal leakage coefficient, piston stroke of servo cylinder, initial position of servo cylinder piston, effective bulk modulus and total mass converted to the servo cylinder piston, their proportions of two sensitivity indexes are relatively small with displacement step values change and load force change, so these parameters have few effects on displacement output response. The proportions of two sensitivity indexes of conversion factor are relatively large and basically remain unchanged.

(3) For natural frequency of servo valve, damping ratio of servo valve, displacement sensor gain, proportional gain and servo valve gain, their proportions of two sensitivity indexes are all inversely proportional to displacement step values approximately but have little relationship with the load.

(4) For supply oil pressure and load force, their proportions of two sensitivity indexes increase with the increasing of initial load, but the conclusion of servo cylinder piston area is just opposite. However these three parameters proportions of two sensitivity indexes all have little relationship with displacement step value.

(5) For load stiffness and viscous damping, their proportions of two sensitivity indexes are significantly affected by the load, and they increase with the increasing of displacement step value under no load rather than change under load.

More illustrations: the conclusions above are applicable to the nine working conditions mentioned in this paper and the hydraulic drive unit which has the similar structure parameters, but when the working conditions and structure parameters varies, the corresponding conclusions may have a little differences from those in this paper, however, the mathematical model and analysis algorithm of sensitivity analysis can be taken as the general guidance to analyze the parameters sensitivity of the similar system.

References

[1] WANG Lipeng, WANG Junzheng, WANG Shoushen, et al. Strategy of foot trajectory generation for hydraulic quadruped robots gait planning[J]. *Journal of Mechanical Engineering*, 2013, 49(1): 39–44. (in Chinese)

[2] CLAUDIO Semini. *HyQ-design and development of a hydraulically actuated quadruped robot*[D]. Liguria, Italy: University of Genoa, 2008.

[3] VO GIA LOC, IG MO KOO, TRAN DUC TRONG, et al. Sensing and control of quadruped walking and climbing robot over complex environment[C]//*International Conference on Intelligent Robots and Systems, Acropolis Convention Center*, Nice, France, September 22–26, 2008: 3884–3889.

[4] DING Lianghong, WANG Runxiao, FENGHuashan, et al. Brief analysis of a Big Dog quadruped robot[J]. *China Mechanical Engineering*, 2012(5): 505–514.

[5] SONG Xiaomeng, KONG Fanzhe, ZHAN Chesheng, et al. Parameter identification and global sensitivity analysis of Xin'anjiang model using meta-modeling approach[J]. *Water Science and Engineering*, 2013, 6(1): 1–17.

[6] JIM W, HALL, SHAWN A, BOYCE, et al. Sensitivity analysis for hydraulic models[J]. *Journal of Hydraulic Engineering*, 2009, 11: 959–968.

[7] MIAO Fengxian, GUO Zhizhong. A survey of sensitivity technique and its application in power systems analysis and control[J]. *Relay*, 2007, 35(15): 72–75.

[8] JIN Yajuan, ZHANG Yimin, ZHANG Yanlin. Analysis of reliability and reliability sensitivity for machine components by mean-value first order saddle point approximation[J]. *Journal of Mechanical Engineering*, 2009, 45(12):102–107. (in Chinese)

[9] WANG Xingang, ZHANG Yimin, WANG Baoyan. Dynamic reliability sensitivity analysis of mechanical components[J]. *Journal of Mechanical Engineering*, 2010, 46(10): 188–193. (in Chinese)

[10] ABOLFAZL ABDOLLAHIPOUR, REZA RAHMANANJED. Sensitivity analysis of influencing parameters in cavern stability[J]. *International Journal of Mining Science and Technology*, 2012(22): 707–710.

[11] ZHOU Yu, ZHANG Zheng, ZHONG Qunpeng. Improved reliability analysis method based on the failure assessment diagram[J]. *Chinese Journal of Mechanical Engineering*, 2012, 25(4): 832–837.

[12] HISKENS I A, PAI M A. Trajectory sensitivity analysis of hybrid system[J]. *IEEE Trans on Circuits and Systems*, 2000, 47(2): 204–220.

[13] LIU Wei, CAO Gang, ZHAI Hongbo, et al. Sensitivity analysis and dynamic optimization design of supports' positions for engine pipelines[J]. *Journal of Aerospace Power*, 2012, 27(12): 2756–2762.

[14] VILENIUS M J. The application of sensitivity analysis to electrohydraulic position control servos[J]. *Journal of Dynamic Systems, Measurements and Control*, 1983, 105: 77–82.

[15] FTARASA S, AJAM H. Sensitivity analysis of parameter changes in nonlinear hydraulic control systems[J]. *International Journal of Engineering*, 2005, 18(3): 239–252.

[16] KONG Xiangdong, YU Bin, QUAN Lingxiao, et al. Trajectory sensitivity analysis of hydraulic drive unit of quadruped bionic robot[J]. *Journal of Mechanical Engineering*, 2013, 49(14): 170–175. (in Chinese)

[17] LI Hongren, GUAN Guangfeng, GUO Hongbo, et al. Modeling, Simulation and experiment on valve controlled asymmetry piston considering valve port error[J]. *Chinese Journal of Mechanical Engineering*, 2007, 43(9): 33–39. (in Chinese)

[18] ZHAO Jianhua, GAO Dianrong. Dynamic characteristic comparison of open-type hydrostatic worktable both before and after linearization[J]. *Journal of Mechanical Engineering*, 2012, 48(24): 158–163. (in Chinese)

Biographical notes

KONG Xiangdong, born in 1959, is currently a professor at *Yanshan University, China*. He received his PhD degree from *Yanshan University, China*, in 1988. His main research interests include electro-hydraulic servo control system and Heavy machinery fluid transmission and control.
Tel: +86-335-8051166; E-mail: xdkong@ysu.edu.cn

YU Bin, born in 1985, is currently a lecture at *Yanshan University, China*. His research interest is fluid transmission and control.
E-mail: yb@ysu.edu.cn

QUAN Lingxiao, born in 1976, is currently a A.D. at *Yanshan University, China*. His research interest is electro-hydraulic servo control system.
E-mail: lingxiao@ysu.edu.cn

BA Kaixian, born in 1989, is currently a PhD candidate at *Yanshan University, China*. His research interest is modeling in servo control system.
E-mail: 315766026@qq.com

WU Liujie, born in 1989, is currently a master candidate at *Yanshan University, China*. His research interest is redundant force restraining of load simulation system.
E-mail: 837010219@qq.com